On the Spectral Similarities between 1,2,6,7-Tetracyano-3,5-dihydro-3,5-diiminopyrrolizinato Complexes and Phthalocyanines – X-ray Crystal and Molecular Structure of Two Mixed Monopyrrolizinato Nickel(II) Complexes with the 2,4-*tert*-Butylacetylacetonide Ligand

Alberto Flamini,*[a] Vincenzo Fares,*[a] and Augusto Pifferi[b]

Keywords: Pyrrolizinato complexes / Tetracyanoethylene / Phthalocyanines

Complexes of Ni^{II}, Cu^{II}, Zn^{II}, and Co^{III} containing the 1,2,6,7-tetracyano-3,5-dihydro-3,5-diiminopyrrolizinide (L) and the 2,4-*tert*-butylacetylacetonide (DPM) ligands have been synthesized and characterized. The absorption optical spectra of these species and of the corresponding ML_2 complexes in coordinating solvents are compared with those of metal-phthalocyanines (MPc) and hydrogen-phthalocyanine (H_2Pc), respectively. The comparison shows a close similarity, especially for the nickel-containing species, in the low-energy spectral region where the first $\pi\rightarrow\pi^*$ transitions occur (Q band). The Q band position of the pyrrolizinato complexes is much more dependant on the metal than is the case for MPc. For the same metal, the Q band position is also dependant on the M–N bond lengths in the molecular plane. For M = Ni, a reduction of this distance causes a red-shift of the Q band and a decrease of its maximum intensity. These conclusions are based on the X-ray molecular structure of the solvent-free NiL(DPM) complex and its pyridine solvate NiL(DPM)$(Pyr)_2 \cdot 2$ Pyr and on their solvatochromism. A symmetry-based correlation diagram between the frontier orbitals of the pyrrolizinato-complexes and the phthalocyanines is proposed.

Introduction

During the last ten years, we have been investigating the metal(II) complexes of the ligand (L) 1,2,6,7-tetracyano-3,5-dihydro-3,5-diiminopyrrolizinide, a derivative of tetracyanoethylene (TCNE) (Scheme 1). Our attention was mainly concentrated on the structurally characterized bis-pyrrolizinates ML_2 (ML_2 = Fe,[1] Co,[1] Ni,[2] Cu,[3] Zn,[4] and Pd[5]). An important feature of these species is the surprisingly strict similarity of their optical spectra (due to the $\pi\rightarrow\pi^*$ transitions), especially in the low-energy region (Q band), with those of metal-phthalocyanines (-tetraazatetrabenzoporphyrins, MPc). This allows ML_2 complexes to be used as spectroscopic models, potentially for better understanding the electronic structure of porphyrinic systems. This is in spite of the deep structural dissimilarities and differences in the number of π-orbitals and π-electrons between the two systems. Recently, the optical spectrum of FeL_2 was assigned in D_{2h} symmetry by using polarized specular reflectance measurements on single crystals of its tetrahydrofuran (THF) adduct, $FeL_2 \cdot 4$ THF.[6] Well-resolved solid-state optical spectra, in close agreement with the solution spectra, were obtained. Interestingly, it was found that the Q band in this system originates from four different electronic transitions [$Q_{(x)}$, $Q'_{(y)}$, $R_{(x)}$, $R'_{(y)}$]. So, it was concluded by analogy that the same band in the MPc's (D_{4h}) should be composed of two electronic transitions [$Q_{(x,y)}$, $R_{(x,y)}$]. This conclusion is in contrast with the widely accepted and supposedly well-established assignment, based on Gouterman's model, where the Q band in MPc's is due to a single electronic transition plus a vibronic component.[7–9] We sometimes also isolated a few monopyrrolizinates (ML), specifically [Cl_2PdL^-][10] and CH_3HgL,[11] but because of the lack of suitable single crystals, we were not able to characterize them using X-ray analysis. However, the optical spectrum of these species are also close to those of the corresponding MPc, even closer than the analogous ML_2. On these grounds, we were interested in synthesizing and characterizing a series of homologous monopyrrolizinates, and to compare their optical spectra with those of the series ML_2 and MPc in order to define

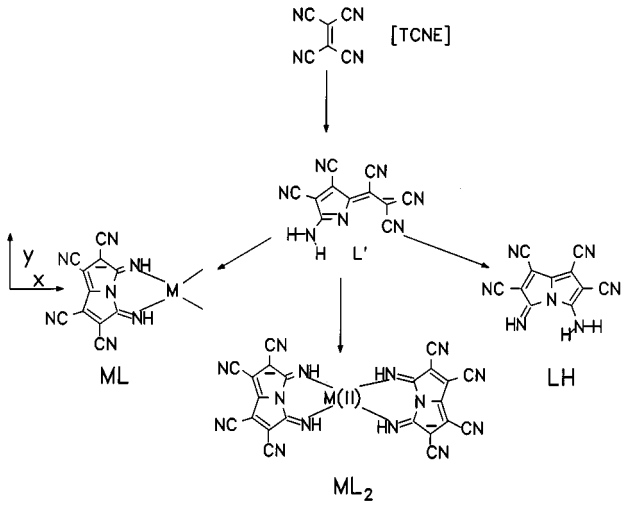

Scheme 1. Relationships between tetracyanoethylene and its derivatives L′, ML, LH, ML_2

[a] Istituto di Chimica dei Materiali del CNR, Area della Ricerca di Roma,
P. O. Box 10, 00016 Monterotondo Stazione (Roma), Italy
[b] Istituto di Strutturistica Chimica del CNR, Area della Ricerca di Roma,
P. O. Box 10, 00016 Monterotondo Stazione (Roma), Italy

  1434–1948/00/0303–0537 $ 17.50+.50/0

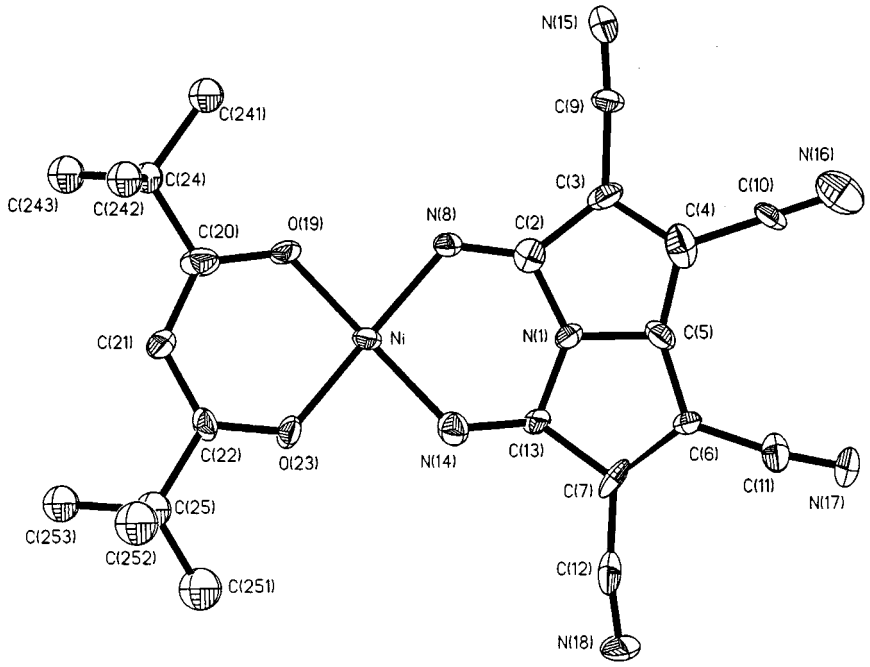

Figure 1. Molecular structure and labelling scheme of NiL(DPM). Thermal ellipsoids are at 30% of probability level

more precisely the significant spectral similarities within the ML series in comparison to the others and, at the same time, to provide further experimental data for an overall rationalization based on molecular orbital calculations. We then found that the acetylacetonide ligand (acac) may coexist with L in coordinating the same metal center for several metals (M = Co, Ni, Cu, Zn). More importantly, the 2,4-*tert*-butyl-derivative of acac (or dipivaloylmethanide, DPM) made it possible to isolate single crystals, suitable for the X-ray structure determination, of the complexes NiL(DPM) and the corresponding pyridine (Pyr) solvate NiL(DPM)$(Pyr)_2 \cdot 2$ Pyr. Furthermore, NiL(DPM) shows an exceptional solvatochromism in solution, varying the coordination properties of the solvent. The available structural data of these nickel complexes suggest that this phenomenon is due to a variation of the Q band in both energy and intensity, and is related to the variation of the Ni–N equatorial distances. We report here on all these findings.

Table 1. Selected bond lengths [Å] and angles [°] for compound **1**

Ni–N(8)	1.884 (8)	N(8)–Ni–N(14)	95.0(4)
Ni–N(14)	1.893 (9)	O(19)–Ni–O(23)	95.3(3)
Ni–O(19)	1.833 (7)	C(2)–N(1)–C(13)	132.2(7)
Ni–O(23)	1.848 (7)	N(1)–C(2)–N(8)	123.4(10)
N(1)–C(2)	1.376 (16)	Ni–N(8)–C(2)	122.1(7)
N(1)–C(5)	1.398 (8)	Ni–N(14)–C(13)	129.7(7)
N(1)–C(13)	1.382 (15)	N(1)–C(13)–N(14)	115.1(9)
C(2)–C(3)	1.468 (16)	Ni–O(19)–C(20)	127.5(7)
C(2)–N(8)	1.287 (13)	O(19)–C(20)–C(21)	121.5(11)
C(3)–C(4)	1.401 (16)	C(20)–C(21)–C(22)	126.0(9)
C(4)–C(5)	1.389 (18)	C(21)–C(22)–O(23)	123.9(10)
C(5)–C(6)	1.387 (16)	Ni–O(23)–C(22)	124.9(7)
C(6)–C(7)	1.396 (14)		
C(7)–C(13)	1.480 (14)		
N(14)–C(13)	1.290 (14)		
O(19)–C(20)	1.310 (15)		
C(20)–C(21)	1.378 (19)		
C(20)–C(24)	1.522 (18)		
C(21)–C(22)	1.376 (18)		
C(22)–O(23)	1.303 (13)		
C(22)–C(25)	1.517 (18)		

Results and Discussion

Synthesis and Structures of ML(DPM)

The monopyrrolizinates are readily formed from the reaction between LH and the bisacetylacetonates. This is not the case when using ML_2 as the pyrrolizinido source for the same reaction. Nevertheless, they are fairly stable towards the ligand metathesis, so that they could all be purified by recrystallization from hot saturated solutions. In any case, the pyrrolizinide moiety is planar and, with respect to DPM, either coplanar as in the Ni^{II} complexes (see later) or rotated by 90° as in ZnL(DPM) · 3 NAPH.[12] The complex CoL(DPM), if it exists, was not isolated. The reaction between LH and $Co(DPM)_2$, even under a rigorously controlled inert atmosphere, always gives a mixture of Co^{II} and Co^{III} complexes, characterized by a visible spectrum with two intense absorption maxima at 636 and 714 nm, respectively. Therefore, only the Co^{III} complex can be isolated as a pure species from the above reaction, provided that this is carried out under the appropriate conditions. A mild oxidizing agent (air) in a poorly Co^{II}-coordinating solvent (acetonitrile) was enough to achieve this. The complex $CoL(DPM)_2$ was therefore synthesized, and it could be recrystallized as a solvent-free species from hot toluene in air without decomposition.

X-ray Structure of the Solvent-Free NiL(DPM)

The molecular structure is shown in Figure 1. Selected bond lengths and angles are reported in Table 1. The nickel

atom is four-coordinate as NiN_2O_2 in a slightly distorted square-planar geometry with two imino-groups from the pyrrolizinido ligand (L) and two oxygen atoms from DPM. The Ni–N and Ni–O mean distances, of 1.889(8) and 1.840(9) Å respectively, are very close to the corresponding ones in the parent bis-chelate square-planar complexes NiL_2[13] and $Ni(DPM)_2$.[14] Also, the geometrical parameters within the two ligands L and DPM are similar to those of the above mentioned bis-chelates. This is different for the bis-pyrrolizinato NiL_2 complexes, in which two donor solvent molecules, doubly hydrogen-bonded to the chelating imino groups in the equatorial plane, are always present,[2,13] and no "equatorial adduct" is formed.

The NiL(DPM) molecule is essentially planar, the best plane being orthogonal to the (010) plane and is almost coincident with the crystallographic (–103) plane. The major molecular axis **x**, defined as the line passing through N(1), Ni, and C(21) atoms, makes angles of 35 and 62° with the *a* and *c* axes respectively, while the minor molecular axis **y**, normal to **x** through Ni in the plane, is parallel to *b*. The crystal structure of NiL(DPM) consists therefore of parallel, iso-oriented, solvent-free complex units, with only weak intermolecular interactions: symmetry-related molecular units weakly interact via –CN···HN– hydrogen bonds (N···H distances in the range 2.18–2.32 Å) developing along the *y* crystallographic direction.

X-ray Structure of NiL(DPM)(Pyr)$_2$ · 2 Pyr

The molecular structure is shown in Figure 2' and is strictly related to **1** decribed above. The nickel atom is in a distorted octahedral geometry NiN_4O_2, with two pyridine molecules axially coordinated at a distance Ni–N_{ax} of 2.117(9) Å (av.), whose planes are rotated 90° with respect to each other, bisecting the N(8)–Ni–N(14) and N(8)–Ni–O(19) angles, respectively. The Ni–N and Ni–O equatorial distances, of 2.084(12) and 2.004(11) Å respectively, are similar to those found in analogous octahedral nickel(II) complexes,[2,15] and longer by ca. 0.19 and 0.16 Å respectively than the corresponding values in the square-planar NiL(DPM). Also, the geometrical parameters of the two ligands L and DPM, although affected by high e.s.d.'s because of the presence of two interstitial solvent pyridine molecules in the asymmetric unit (each one disordered at two slightly different positions), are very similar to those found in **1** (see Table 2). As regards the crystal packing, it is noteworthy that the Ni–N_{ax} vector, the major molecular axis **x**, and the minor molecular axis **y** are parallel to *b*, *a*, and *c* respectively. Therefore, parallel iso-oriented molecular units are therefore also found, with weak intermolecular hydrogen-bonds (–CN···HN– in the range 2.56–2.64 Å) forming a monodimensional network along the *z* direction.

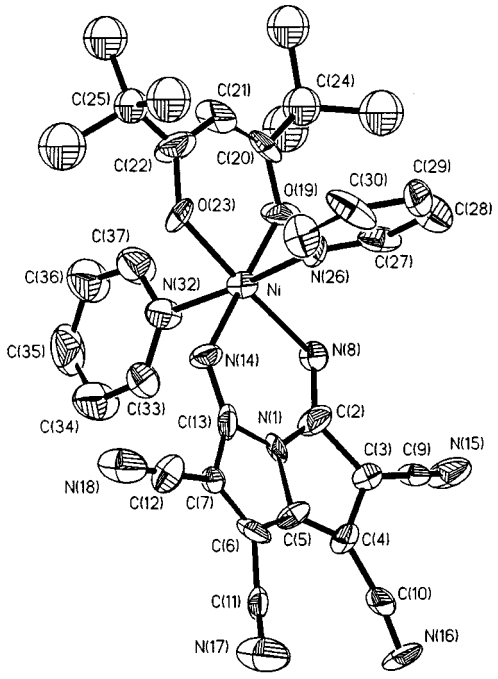

Figure 2. A perspective view of the complex NiL(DPM)(Pyr)$_2$ · 2 Pyr with the numbering scheme. The two disordered pyridine solvent molecules are not shown. Thermal ellipsoids are at 30% probability level

Table 2. Selected bond lengths [Å] and angles [°] for compound **2**

Ni–N(8)	2.089 (11)	N(8)–Ni–N(14)	91.0(4)
Ni–N(14)	2.079 (12)	O(19)–Ni–O(23)	91.4(4)
Ni–O(19)	2.007 (10)	N(26)–Ni–N(32)	176.2(6)
Ni–O(23)	2.001 (9)	C(2)–N(1)–C(13)	134.4(10)
Ni–N(26)	2.114 (8)	N(1)–C(2)–N(8)	124.6(13)
Ni–N(32)	2.120 (7)	N(1)–C(13)–N(14)	120.2(12)
N(1)–C(2)	1.369 (22)	Ni–N(14)–C(13)	126.3(10)
N(1)–C(5)	1.374 (16)	Ni–O(19)–C(20)	122.9(9)
N(1)–C(13)	1.372 (21)	O(19)–C(20)–C(21)	126.5(13)
C(2)–C(3)	1.451 (19)	C(20)–C(21)–C(22)	128.9(12)
C(2)–N(8)	1.291 (16)	C(21)–C(22)–O(23)	120.3(13)
C(3)–C(4)	1.412 (18)	Ni–O(23)–C(22)	129.0(9)
C(4)–C(5)	1.400 (23)		
C(5)–C(6)	1.412 (24)		
C(6)–C(7)	1.392 (21)		
C(7)–C(13)	1.440 (20)		
C(13)–N(14)	1.299 (15)		
O(19)–C(20)	1.302 (18)		
C(20)–C(21)	1.396 (23)		
C(20)–C(24)	1.502 (20)		
C(21)–C(22)	1.386 (22)		
C(22)–O(23)	1.299 (18)		
C(22)–C(25)	1.520 (20)		

We may note that both complexes **1** and **2**, because of their crystallographic features, are good candidates for a spectroscopic investigation using polarized light on single crystals in order to have valuable information on the electronic structure of porphyrins in addition to the data already known from $FeL_2 \cdot 4$ THF.[6]

Optical Spectra of ML(DPM)

These spectra (Figure 3 and Table 3) are characterized by intense bands due to $\pi \rightarrow \pi^*$ electronic transitions localized on the planar system formed by the pyrrolizinido moiety and the adjacent chelate ring including the metal. The low-energy portion of these spectra from the window centered at 500 nm is very similar to that of the corresponding MPc's spectra, except for an enhanced band intensity in the latter. In particular, the Q band profile is amanzingly alike for the

Table 3. Optical spectra [maxima in Kk and (log ε); shoulders in parentheses] of ML(DPM) and ML_2 complexes

NiL(DPM) in CH_2Cl_2	NiL(DPM) in THF	$CoL(DPM)_2$ in THF	CuL(DPM) in THF	ZnL(DPM) in THF	NiL_2 in CH_3OH	CoL_2 in THF	CuL_2 in THF	ZnL_2 in THF
13.19 (4.06)	14.90 (4.65)	14.14 (4.39)	15.08 (4.56)	15.13 (4.63)	15.29 (4.91)	15.72 (4.70)	15.31 (4.65)	14.97 (4.83)
14.60 (3.78)	[15.36] (4.17)	15.58 (3.96)	16.39 (4.18)	[15.58] (4.32)	16.26 (4.74)	16.61 (4.54)	16.13 (4.63)	15.36 (4.70)
[16.08] (3.46)	16.34 (4.11)	[17.04] (3.49)	[17.79] (3.63)	16.47 (4.17)	[16.81] (4.49)	[17.18] (4.30)	[16.67] (4.36)	16.31 (4.56)
[20.62] (3.99)	[17.04] (3.65)			[17.04] (3.86)	17.64 (4.16)	17.95 (4.01)	[17.54] (4.00)	[16.81] (4.30)
	[17.73] (3.46)			[17.86] (3.56)	[18.28] (3.93)			[17.70] (3.99)
								[18.35] (3.78)
22.47 (4.00)	24.45 (3.94)	24.39 (4.03)	25.38 (4.09)	25.44 (3.96)	24.45 (4.37)	25.25 (4.16)	25.38 (4.33)	25.19 (4.29)
[24.69] (3.81)	[25.84] (3.79)	[25.64] (3.91)	[26.67] (3.98)	[26.67] (3.83)	[25.84] (4.19)	[26.67] (4.01)	[26.67] (4.16)	[26.52] (4.15)
[29.24] (3.68)		[29.41] (3.97)						[28.82] (3.92)
[32.05] (4.01)	[32.05] (4.20)	34.48 (4.37)	[31.75] (4.26)	[32.79] (4.21)	[33.33] (4.25)	[32.05] (3.81)	[34.25] (4.34)	[33.33] (4.31)
[35.46] (4.13)	32.68 (4.21)		32.68 (4.34)	33.78 (4.38)	36.36 (4.41)	[33.90] (4.08)	36.76 (4.48)	36.36 (4.42)
39.06 (4.45)			36.76 (4.24)	36.76 (4.17)		36.90 (4.20)		

nickel-containing species. It is to be noted, however, that the Q band maximum in the monopyrrolizinates shows a comparatively large dependence on the nature of the metal ion, varying by 47 nm from ZnL(DPM) to $CoL(DPM)_2$. In fact, for MPc's such a trend is almost negligible, being at most 9 nm. More interestingly, in the monopyrrolizinato series, the effect on the Q band can be examined by varying the M–N bond length in the molecular plane for the same M, as detailed in the following section.

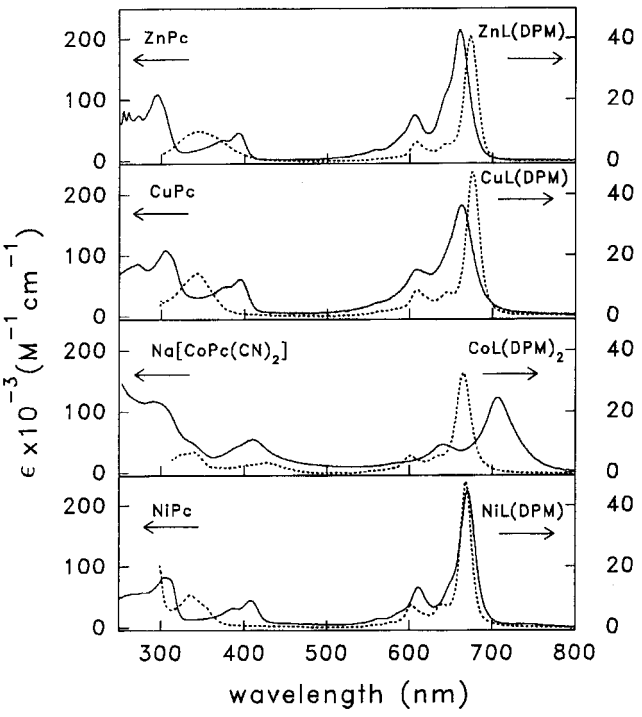

Figure 3. Solution optical spectra of the monopyrrolizinato metal complexes (—— in THF) and the corresponding metalphthalocyanines (- - - - NiPc and CuPc in 1,2,4-trichlorobenzene, Na-[$CoPc(CN)_2$] in acetone, ZnPc in dimethylacetamide)

Solvatochromism and Thermochromism of NiL(DPM)

NiL(DPM) shows an exceptional solvatochromism: its colour is pale-green in an uncoordinating solvent (CH_2Cl_2 or acetone) but becomes an intense blue in a coordinating solvent (THF) or on adding a coordinating species to the uncoordinating solvents, as for examples adding pyridine to CH_2Cl_2 or water to acetone. In Figure 4a, the pertinent spectral changes in question are reported for CH_2Cl_2/pyridine as a solvent system. These changes, being the same for the several solvent systems tested, can be interpreted as resulting from a perturbation of the frontier π orbitals of NiL(DPM) by axial coordination to the nickel atom. From the X-ray molecular structural parameters available, we can state that an elongation of the Ni–N bond in the molecular plane causes a sharpening, a blue shift, and an increase of the maximum intensity of the Q band. The change of the coordinating properties of the solvent also results in a different coordination geometry around the nickel ion, from square planar to octahedral, with an associated different optical metal d→d transition pattern.[16] However, such transitions are comparatively much weaker than the π→π* transitions, since their molar absorbitivities are in the range 1–100 $M^{-1}\cdot cm^{-1}$.[17] So, it can be concluded that the observed solvatochromism, which involves optical bands with molar absorbitivities in the range 10^4 $M^{-1}\cdot cm^{-1}$ (Table 3), originates from a conformational change of the π electron systems rather than by the difference in the metal coordination.

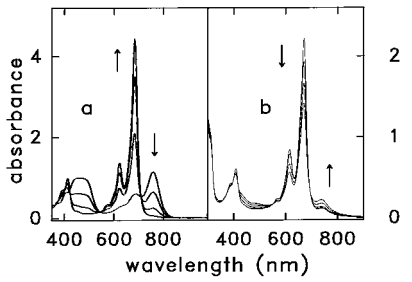

Figure 4. (**a**) Spectral changes of a dichloromethane solution of NiL(DPM) (3.0 mL, $C = 9.91\cdot10^{-5}$ M, pathlength = 1 cm) on adding increasing amounts (0.7, 1.7, 4.7 mL) of pyridine in CH_2Cl_2 (0.005 M). (**b**) Spectral changes of a THF solution of NiL(DPM) ($C = 6.03\cdot10^{-5}$ M, pathlength = 1 cm) on heating: 22, 40, 60, 75 °C. In both **a** and **b**, the arrows indicate the direction of the spectral changes

Moreover, NiL(DPM) in a coordinating solvent (e.g. THF) is thermochromic (Figure 4b). This phenomenon can be reasonably explained as solvatochromism. That is, by decreasing the temperature, the equilibrium in solution, NiL(DPM) · 2 THF $\rightleftarrows$ NiL(DPM) + 2 THF, shifts to the left. Therefore, the resulting spectral changes parallel those occurring on adding pyridine to NiL(DPM) in CH_2Cl_2.

For completeness, we ascertained that all other monopyrrolizinato complexes are neither solvatochromic nor thermochromic, including the isomorphous CuL(DPM). In this case, the reason for the absence of any solvatochromism, despite the well-known tendency of square-planar Cu^{II} complexes to increase the metal-coordination number, might be that the Cu–N_{eq} distances do not lengthen significantly, due to the large Jahn–Teller effect normally observed in these type of compounds,[3,18] on going from square-planar to tetragonally elongated hexa-coordination.

Optical Spectra of ML_2

We previously[1–4] reported the solution optical spectra of ML_2 complexes, but, for the reasons given below, most of these data actually referrred to ML species. Here, the correct spectra of the pertinent ML_2 species are presented for the first time (Figure 5 and Table 3). The resemblance of these spectra, particularly that of NiL_2, to the spectrum of H_2Pc is to be noted, within the limits already outlined in comparing ML(DPM) and MPc. This resemblance is now less surprising than in the previous interpretation, given that the two systems display the same symmetry (D_{2h}). We therefore conclude that the spectral changes occurring upon lowering the symmetry from D_{4h} to D_{2h} in tetraazatetrabenzoporphyrins are the same as those occurring when going from ML to ML_2, and that the resulting Q-band splitting is similar (0.8–1.0 Kk) in either case for M = Ni.

We now explain why the previously reported spectra of ML_2 were not interpreted correctly. Actually, the previous spectra were those of ML since they were recorded in solution with excess metal ion (M). Recently, we ascertained that an excess of free metal ion in solution in the presence of L' or ML_2 stabilizes the mono-pyrrolizinato species as a consequence of the reaction: ML_2 + M $\rightleftarrows$ 2 ML. The spectral changes associated with this reaction were recorded for M = Ni in methanol and methanol/THF as solvents. In both solvent systems, the initial and final spectra are the same, while the dynamics are different. The process is slower in methanol and can be easily followed at room temperature (Figure 6). From the presence of several isosbestic points it is clear that only one clean reaction occurs, and that the reaction product is the monopyrrolizinato-complex NiL, since the final spectrum is the same as that of NiL(DPM) (see Figure 3), except for the $\pi\rightarrow\pi^*$ electronic transitions (falling below 320 nm) localized on DPM in the latter.

Other noteworthy features of ML_2 spectra are, as in the ML(DPM) series, the dependence of the Q band maximum both on the metal ion (Table 3) and on the M–N bond length for constant M. Again, for M = Ni the consequent solvatochromism and thermochromism have been observed

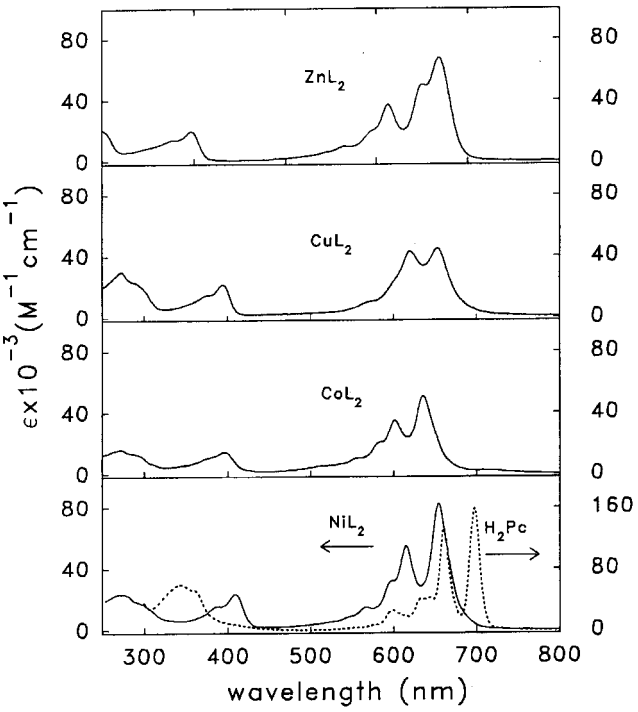

Figure 5. Solution optical spectra of bis-pyrrolizinato metal complexes (—— NiL_2 in CH_3OH, CoL_2, CuL_2, and ZnL_2 in THF) and of hydrogenphthalocyanine (- - - - in 1,2,4-trichlorobenzene)

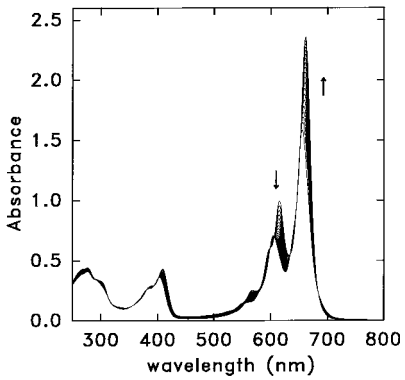

Figure 6. Spectral changes with time (every 5 min) undergone by a CH_3OH solution of NiL_2 (C = $1.96\cdot10^{-4}$ M) after addition of 200 molar equivalents of $NiCl_2 \cdot 6\,H_2O$

in nitrobenzene/pyridine and ethyl acetate[19] as the solvent system, respectively.

Hypothesis on the Electronic Structure of ML Complexes

On the basis of the current solution spectral data, together with those from FeL_2, for which a close agreement between solution and solid state spectra was found, a correlation diagram of the frontier orbitals can be constructed for the MPc, H_2Pc, ML_2, and ML series, (Figure 7) and a reasonable hypothesis about the electronic structure of ML complexes can be put forward. This correlation diagram is presented in Figure 7. In ML_2 or H_2Pc (D_{2h}), four transitions give rise to the Q band. In MPc (D_{4h}) these transitions are reduced to two by symmetry.

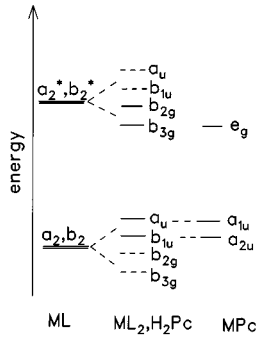

Figure 7. Qualitative scheme of the frontier orbitals for the systems ML, ML_2 or H_2Pc, and Mpc

Now, because of the similarity between ML and MPc, we must also suppose that the Q band is in ML is also composed of two electronic transitions involving MPc-like orbitals. In a C_{2v} molecule such as ML (Scheme 1), the π-molecular orbitals are of a_2 or b_2 symmetry and there is no forbidden π→π* transition, being $a_2 \rightarrow a_2$ or $b_2 \rightarrow b_2$ *x*-allowed and $a_2 \rightarrow b_2$ *y*-allowed. So, the frontier orbitals of ML could be two HOMO's (a_2, b_2) and two LUMO's (a_2*, b_2*), both nearly degenerate. The four excited electronic states, 2 A_1 and 2 B_1, originating from the transitions among these orbitals could be reduced to two after a configuration interaction: A_1 and B_1, consisting of the mixed configurations $a_2 \rightarrow a_2$*/$b_2 \rightarrow b_2$* and $a_2 \rightarrow b_2$*/$b_2 \rightarrow a_2$*, respectively. Furthermore, this orbital pattern in ML is consistent with the frontier orbitals in ML_2. Here, the π-ligand orbitals can be considered as the symmetric and antisymmetric combinations of the corresponding orbitals of two ML weakly interacting fragments. As a matter of fact, the b_{3g} and a_u in D_{2h} are the symmetric and antisymmetric combination of a_2 in C_{2v}, while b_{1u} and b_{2g} are the corresponding combinations of b_2, respectively.

Conclusions

The optical spectra similarity between the pyrrolizinates and the phthalocyanines has been further studied: the spectra of ML_2 are similar to H_2Pc, and the increase of symmetry by switching from H_2Pc to MPc is spectrally equivalent to removing a pyrrolizinato moiety from ML_2. The origin of such similarity, in spite of the many differences between the two systems, still awaits an explanation and it will probably be accounted for only with appropriate molecular orbital calculations based mainly on the current experimental data. In the pyrrolizinates, the metal ion effect on the optical spectrum is much larger than in the phthalocyanines, so that the closest resemblance occurs for M = Ni and when Ni–N is relatively long (2.08 Å), in both ML and ML_2 series. The Ni-pyrrolizinates made it possible to see the effect on the electronic spectrum while varying the Ni–N bond length in the molecular plane. This effect is responsible for both the solvatochromism and the thermochromism in these species, while is not seen in the phthalocyanines because of the rigidity of the metal-coordinating hole size. Both title Ni–monopyrrolizinato species display a crystal structure suitable for spectroscopic investigation with polarized light, which is in progress. Therefore, additional experimental information on the electronic structure of these systems, valuable also for porphyrinic systems, will be available in the near future.

Experimental Section

Materials: Our procedures were followed for the synthesis of LH[20] and ML_2 (M = Co,[1] Ni,[2] Cu,[3] Zn[4]), while $M(DPM)_2$ (M = Co, Ni, Cu, Zn),[21] $Co(DPM)_3$[21] and $Na[CoPc(CN)_2]$[22] were prepared as described in the literature. Commercial H_2Pc, NiPc, CuPc, and ZnPc were purified by sublimation. Pyridine, CH_3CN, CH_3OH, THF, toluene, acetone, and CH_2Cl_2 were dried and freshly distilled before use. 1-Chloronaphthalene (NAPH) was used as received from Fluka.

General Procedures: Microanalyses were by Malissa and Reuter Analytische Laboratorien, Elbach, Germany, and by Servizio Microanalisi del CNR, Area della Ricerca di Roma. – Solution optical spectra were recorded on a Cary 5 and IR spectra on a Perkin–Elmer 16F PC FT spectrometer on Nujol mulls. – The magnetic measurements were carried out by using the Gouy method at room temperature. Molar susceptibilities were corrected for intrinsic diamagnetism estimated from Pascal's constants. – Suitable single crystals of ML for X-ray crystallography were grown in a sealed vial from a hot saturated solution of the sample in the appropriate solvent, followed by slow cooling, over several days, from the reflux temperature of the solvent down to room temperature (RT) in an ASCON M710 thermostatic oven.

Preparation of NiL(DPM): $Ni(DPM)_2$ (0.420 g, 0.985 mmol) was dissolved in methanol (60 mL) and LH (0.174 g, 0.746 mmol) added. After 1 h stirring a grey microcrystalline solid precipitated leaving a light-blue solution behind. After filtration, the solid was washed with methanol and dried in air. Yield 0.313 g (0.66 mmol, 88%). Diamagnetic: $\chi_M = -237 \cdot 10^{-6}$ e.m.u. – $C_{22}H_{21}N_7NiO_2$: calcd. C 55.73, H 4.46, N 20.68, Ni 12.38, O 6.75; found: C 56.77, H 4.30, N 21.10. Single crystals were obtained in a vial from a toluene/acetone (7:3) mixture, on cooling from 70 °C to room temp. over 15 d.

Crystal Growth of NiL(DPM)(Pyr)$_2$ · 2 Pyr: A suspension of NiL(DPM) (0.1 g) in a toluene/pyridine mixture (90:10, 30 mL) was heated under reflux, under N_2 for 30 min. The hot saturated solution was filtered and sealed in a vial under vacuum. On cooling the vial from 95 °C to room temp. over 20 h purple needle-like crystals of the NiL(DPM)–tetrapyridinate separated. This compound loses pyridine quite rapidly in air so that all the solid-state measurements on it were not reproducible, apart from the single crystal X-ray diffraction data, provided that the crystals were exposed to a saturated vapour of their mother liquor.

Preparation of CuL(DPM): $Cu(DPM)_2$ (1.930 g, 4.48 mmol) was dissolved in CH_3CN (80 mL) and LH (0.500 g, 2.15 mmol) added. An intense blue coloured solution was immediately formed. This solution was left 4 h at room temp. and then chilled down to –20 °C. A purple microcrystalline solid separated, which was filtered at low temperature and then dried in air. Yield 0.620 g, (1.29 mmol, 60%). Paramagnetic: $\mu_{eff} = 1.72\ \mu_B$. – $C_{22}H_{21}CuN_7O_2$: calcd. C 55.18, H 4.42, N 20.47, Cu 13.25, O 6.68; found: C 55.09, H 4.29,

N 21.51. Single crystals were obtained in a vial from a toluene/CH_3CN (7:3) mixture, on cooling from 90 °C to room temp. over 3 d and then leaving the sample at this temperature for another 10 d. This compound is isomorphous to the analogous NiL(DPM).[23]

Table 4. Crystallographic data for NiL(DPM) (**1**) and NiL(DPM)$(Pyr)_2 \cdot 2$ Pyr (**2**)

	1	**2**
Chemical formula	$C_{22}H_{21}N_7NiO_2$	$C_{42}H_{41}N_{11}NiO_2$
Molecular weight	474.2	790.6
Crystal size [mm]	1.0 × 0.1 × 0.01	0.3 × 0.3 × 0.3
X-ray source	HXD Elettra	Rotating anode
Data coll apparatus	Image Plate Area Det	Rigaku 4-circle Diffr
Data coll temp [K]	293	296
Crystal system	Monoclinic	Orthorhombic
Space group	$P2_1$ (No. 4)	$Pna2_1$ (No. 33)
Cell parameters [Å]	a = 5.901(3)	20.374(3)
	b = 18.275(9)	12.597(1)
	c = 10.288(4)	18.021(1)
	β = 96.81°	
V [Å^3]	1101.7(9)	4625.1(8)
Z	2	4
Density (calc.) [g cm^{-1}]	1.429	1.135
λ [Å]	0.75500	1.5418
Absorption coefficient [mm^{-1}]	0.915	0.958
No. collected data	9218	3444
No. unique reflections	2135	1948
R_{merge}[a]	0.075	0.070
No. observed reflections	1325[$F_o \geq 4\sigma(F_o)$]	1599 [$F_o \geq 6\sigma(F_o)$]
R indices[b]	R = 6.6%, R_w = 8.2%	R = 7.4%, R_w = 10.2%
GOF	1.09	1.04

[a] $R_{merge} = \Sigma_h \Sigma_i(\mid Ih,i - \langle Ih \mid \rangle)/\Sigma_h \Sigma_i Ih,i$ where Ih,i is the intensity value of the i^{th} measurement of h and $\langle Ih$ is the corresponding mean value of h for all i measurements of h. – [b] $R = \Sigma(\mid F_o - F_c \mid)/\Sigma|F_o|$. $R_w = [\Sigma_w(F_o - F_c)^2/\Sigma_w \mid F_o \mid ^2]^{1/2}$.

Preparation of ZnL(DPM) · 3 NAPH: $Zn(DPM)_2$ (1.119 g, 2.58 mmol) was dissolved in NAPH (40 mL). This solution was filtered and then LH (0.3 g, 1.29 mmol) added. After stirring the resulting suspension overnight under N_2, the microcrystalline solid in the reaction mixture changed colour from golden (LH) to purple. This solid was collected, washed with light petroleum and dried in air. It was then recrystallized from hot (120 °C) NAPH. The elemental analysis of this compound was not reproducibile, due to the partial loss of NAPH on drying it. Nevertheless, it was possible to ascertain its true composition by means of X-ray crystallography.[12]

Preparation of CoL(DPM)$_2$ $Co(DPM)_2$ (0.712 g, 1.67 mmol) was dissolved in CH_3CN (100 mL) and LH (0.400 g, 1.72 mmol) added. After stirring in air for 5 d at room temp., the resulting dark-green solution was evaporated to dryness. The residue was dissolved in boiling toluene. After filtration and cooling to room temp. the toluene solution afforded dark-green needle-like crystals. Yield 0.600 g (0.91 mmol, 55%). Diamagnetic: $\chi_M = -455 \cdot 10^{-6}$ e.m.u. – $C_{33}H_{40}CoN_7O_4$: calcd. C 60.27, H 6.13, N 14.91, Co 8.96, O 9.73; found: C 60.23, H 6.37, N 14.74, Co 9.02, O 9.95. Attempts to synthesize this compound from $Co(DPM)_3$ were unsuccessful due to the kinetic inertness of this species.

X-ray Crystallography of NiL(DPM) (1) and NiL(DPM)$(Pyr)_2 \cdot 2$ Pyr (2): Compound **1** crystallizes as dark-green needle-like platelets, stable in air, with one of the crystal dimensions being only some microns. In order to obtain a diffraction data set utilizable for an X-ray analysis, it was necessary to use high intensity synchrotron radiation. A well-formed crystal of dimensions 1.0 × 0.1 × 0.01 mm, fixed on a glass fiber, was therefore mounted on the Hard X-Ray Diffraction (HRD) beam-line of ELETTRA (Trieste).[24] Intensity data were collected by using a 16 keV radiation (λ = 0.775 Å) and a 180 mm MAR Image Plate Area Detector, and processed by DENZO[25] and CCP4[26] programs. Unit cell dimensions were determined by mounting the crystal on the Huber four-circle automated diffractometer of the same beam-line and refined from the setting angles of 15 selected high-angle reflections.

The crystals of **2** are unstable in air, leading to the loss of crystallization solvent: a selected crystal was therefore fixed inside a Lindemann capillary in the presence of the mother liquor. Data were collected on a rotating anode AFC5R Rigaku automated diffractometer (Cu-K_α radiation) with a graphite monochromator and corrected for absorption (psi-scan method), Lorentz and polarization effects. Cell constants were refined from setting angles of 22 reflections in the 2θ range 40–80°.

Both structures were solved by direct methods by using the SIR97 programs[27] and refined by full-matrix least-squares methods (248 and 405 variables segmented into two and four blocks for **1** and **2** respectively) by using the SHELXTL programs.[28]

Details of data collection and refinements are given in Table 42. Hydrogen atoms were included using a riding model.

Additional structural diagrams and tables listing atomic coordinates, bond lengths, bond angles, and anisotropic thermal parameters have been deposited with the Cambridge Crystallographic Data Centre under the numbers CCDC-130259 (**1**) and CCDC-130260 (**2**).Copies may be obtained without charge from: CCDC, 12 Union Road, Cambridge CB2 1EZ, UK [fax: +44-1223/336033, E-mail: deposit@ccdc.cam.ac.uk, www: http//www.ccdc.cam.ac.uk].

Acknowledgments

Dr. G. Pochetti for his help in the Image Plate data reduction process, Mr. M. Catricalà and Mr. C. Veroli for technical assistance.

[1] M. Bonamico, V. Fares, A. Flamini, N. Poli, *J. Chem. Soc., Dalton Trans.* **1992**, 3273–3280.
[2] M. Bonamico, V. Fares, A. Flamini, N. Poli, *Inorg. Chem*. **1991**, *30*, 3081–3087.
[3] M. Bonamico, V. Fares, A. Flamini, N. Poli, G. Mattei, *Polyhedron* **1993**, *12*, 1209–1214.
[4] V. Fares, A. Flamini, J. R. Jasin, R. L. Musselman, N. Poli, *J. Chem. Soc., Dalton Trans.* **1995**, 281–286.
[5] M. Bonamico, V. Fares, A. Flamini, N. Poli, *J. Chem. Soc., Dalton Trans.* **1993**, 2073–2074.
[6] C. B. Hoffman, V. Fares, A. Flamini, R. L. Musselman, *Inorg. Chem*. **1999**, *38*, 5742–5748.
[7] M. Gouterman, *J. Mol. Spectrosc*. **1961**, *6*, 138–163.
[8] M. Gouterman, in: *The Porphyrins* (Ed.: D. Dolphin), Academic Press, New York, **1978**, 1–166.
[9] M. Y. R. Wang, B. M. Hoffman, *J. Am. Chem. Soc*. **1984**, *106*, 4235−4240.
[10] A. Flamini, N. Poli, *Polyhedron* **1996**, *15*, 513–518.
[11] A. Flamini, G. Righini, L. Mannina, *Polyhedron* **1999**, *18*, 799–806.
[12] ZnL(DPM) · 3 NAPH crystallizes as dark violet prisms unstable in air. Diffraction data were collected on a selected crystal fixed in a capillary in the presence of mother liquor. Crystal data: monoclinic, $P2_1/c$, a = 10.737(4), b = 26.754(6), c = 17.840(5) Å, β = 102.16(4)°, V = 5009(2) Å^3, Z = 4, D (calc.) = 1.287 g·cm^{-3}. Although the presence of three inde-

pendent highly disordered NAPH molecules did not allow for obtaining accurate structural data, the X-ray analysis showed the Zn complex unit with the metal atom tetrahedrally coordinated to two nitrogen atoms from an L ligand and two oxygen atoms from a DPM ligand at Zn–N and Zn–O mean distances of 1.98 and 1.96 Å, respectively.

[13] M. Bonamico, V. Fares, A. Flamini, N. Poli, Y. Yamashita, K. Imaeda, *J. Chem. Soc., Dalton Trans.* **1993**, 3463–3470.
[14] F. A. Cotton, J. J. Wise, *Inorg. Chem*. **1966**, *5*, 1200–1207.
[15] L. Sacconi, F. Mani, A. Bencini, in: *Comprehensive Coordination Chemistry*, Pergamon Press, **1987**, *5*, 143.
[16] F. A. Cotton, G. Wilkinson, *Advanced Inorganic Chemistry*, 5th ed., Wiley, New York, **1988**, 744–752.
[17] E. Iwamoto, T. Kamamaru, Y. Sumitomo, Y. Suzuki, J. Nishimoto, *J. Chem. Soc., Faraday Trans.* **1995**, *91*, 627–630.
[18] M. Bonamico, V. Fares, A. Flamini, P. Imperatori, N. Poli, *Angew. Chem. Int. Ed. Engl*. **1989**, *28*, 1049–1050.
[19] A. Flamini, N. Poli, *Sensors and Materials*, **1995**, 7, 99–103.
[20] V. Fares, A. Flamini, N. Poli, *J. Am. Chem. Soc.* **1995**, *117*, 11580−11581.
[21] G. S. Hammond, D. C. Nonhebel, C. S. Wu, *Inorg. Chem*. **1963**, *2*, 73−76.
[22] J. Metz, M. Hanack, *J. Am. Chem. Soc*. **1983**, *105*, 828–830.
[23] Crystal data for CuL(DPM); monoclinic, $P2_1$, a = 5.878(1), b = 18.356(9), c = 10.307(5) Å, β = 95.45(3)°, V = 1107(1) Å^3.
[24] S. Bernstorff, E. Busetto, C. Gramaccioni, A. Lausi, L. Olivi, F. Zanini, A. Savoia, M. Colapietro, G. Portalone, M. Camalli, A. Pifferi, R. Spagna, L. Barba, A. Cassetta, *Rev. Sci. Instrum.* **1995**, *66*, 1661.
[25] Z. Otwinowski, W. Minor, in: *Methods in Enzymology* (Eds.: C. W. Carter Jr., R. M. Sweet, Academic Press, San Diego, CA, **1996**, vol. 276.
[26] Collaborative Computational Project, Number 4, *Acta Cryst.* **1994**, *D50*, 760–763.
[27] A. Altomare, M. C. Burla, C. Camalli, G. Cascarano, C. Giacovazzo, A. Guagliardi, A. G. G. Moliterni, G. Polidori, R. Spagna, *J. Appl. Cryst.* **1998**, in press.
[28] G. M. Sheldrick, *SHELXTL*; Siemens: Madison, WI, **1996**, vol 5.

Received August 9, 1999
[I99302]